



OS4-2

Cool Flame Burning During Flame Spread over Droplet Arrays and Clusters

Daniel DIETRICH¹, Vedha NAYAGAM², Forman WILLIAMS³, Masato MIKAMI⁴, Hiroshi NOMURA⁵ and Masao KIKUCHI⁶

- 1 NASA John Glenn Research Center,
- 2 Case Western Reserve University,
- 3 University of California, San Diego,
- 4 Yamaguchi University,
- 5 Nihon University,
- 6 Japan Aerospace Exploration Agency (JAXA)

1. Introduction and Background

Studying isolated droplets and geometrically simplified arrays of droplets is of scientific interest because of the close fidelity of the experiments to theory and also because of the application to spray combustion processes. The combustion of a single droplet dates back to the pioneering work of Godsave¹, with Kumagai² performing the first study in microgravity. Since these early, pioneering studies, single droplet combustion has been the subject of many experimental, theoretical and numerical studies³. A prime reason for this is the geometric simplicity that makes it amenable to detailed theoretical and numerical study. For example, researchers⁴⁻⁶ used the results of recent space-based experiments on droplet combustion to evaluate chemical kinetic mechanisms for pure liquid hydrocarbon fuels, by taking advantage of the spherical symmetry of the problem. These studies all assumed and focused on hot-flame burning and extinction.

Recent experiments aboard the International Space Station (ISS)⁷ showed that, following radiative extinction of the hot-flame surrounding a large alkane droplet, the droplet can continue to burn with a lower temperature cool flame. This cool flame exists because of the negative temperature coefficient (NTC) region of alkane oxidation chemistry. This cool-flame burning has been the subject of a number of subsequent theoretical⁸, numerical^{9,10} and further experimental¹¹ studies.

The next logical step in the understanding of fuel spray combustion is the simplified droplet array¹² and droplet stream¹³. Most previous studies on arrays concentrated on how droplet interactions change the burning rate constant of the droplet. For example, studies in simulated reduced gravity environments^{14,15} and in drop tower experiments¹⁶ observed that the burning rate constant for a droplet array increased as the droplets burned (non-dimensional separation distance increased). The authors explain these results by noting that at smaller inter-droplet spacings, the competition for oxygen results in a decreased burning rate constant. This conclusion is reinforced by simplified theoretical studies of droplet interaction¹⁷.

These droplet array studies focused on the droplet burning rate and flame structure. Further studies¹⁸ showed that droplet interactions promote radiative flame extinction and inhibit diffusive extinction. Since droplet interactions promote radiative extinction (by creating a large envelope flame surrounding the droplet array) and radiative extinction leads to cool flame burning for single alkane droplets, the logical question is whether a droplet array will also burn with a cool flame. Subsequent experiments¹⁹ showed that, in fact, the envelope flame surrounding a binary droplet array will extinguish at a smaller droplet size than a corresponding single droplet and that the array will continue to burn with a cool flame.

While the burning rate has been the most studied parameter in array studies, there is also interest in ignition, extinction and flame spread along a droplet array. Researchers²⁰⁻²² have studied the flame spread along a droplet array with the hope of relating flame propagation in a spray to the flame spread in the simpler geometry. More recent work involved studying the flame spread along a linear array of droplets in microgravity^{23,24}. The goal of the work was to measure both the flame spread rate as a function of inter-droplet separation distance and find the limiting distance where a flame would not spread. These studies were extended to consider the situation where the flame could influence the droplet motion

ahead of it by allowing the droplets to move (nearly) freely in space^{25,26}). The focus was again to determine both the flame spread rate and flame spread limits where the flame can influence the droplet motion.

The focus of the present work is to investigate the flame spread between clusters of droplets and investigate the limits of flame spread between droplet clusters. The work is motivated by the past work on both flame spread over droplet arrays, droplet interactions showing the importance of radiative loss and the discovery of cool-flame burning of droplets undergoing radiative extinction.

2. Experimental Hardware, Diagnostics and Data Analysis

The experiments used the Group Combustion Experiment Module (GCEM) that operated inside the Multipurpose Small Payload Rack (MSPR) located in the Japanese Experiment Module (KIBO) of the International Space Station. The details of the hardware and its operation are provided elsewhere²⁷⁻²⁹), but involved a sealed chamber inside of which was a 30 mm x 30 mm grid of 14 μm SiC fibers spaced 4 mm apart. The experiments reported herein (there were two other investigations performed in the GCEM) examined the flame spread between clusters of droplets. The clusters were arranged in a line with the spacing between clusters increasing with increasing distance from the igniter. The tests involved two configurations of clusters (Fig. 1), two and five droplets in each cluster, with three initial droplet sizes (0.7, 1.0 and 2.0 mm). The experiments operated in three different ambient oxygen mole fractions ($Y_{\text{O}_2} = 0.17, 0.19$ and 0.21) at an ambient pressure of 1.0 atm for all the experiments.

The GCEM experiment hardware provided the primary diagnostic for these experiments - a Canon EOS camera that recorded still images of the droplet array before ignition and then a video view (at reduced spatial resolution) for a period of approximately 70 s spanning a time 10 s before ignition until well after the flame has extinguished and the test was effectively over. The camera was equipped with a backlight that flashed on and off periodically so that the single video

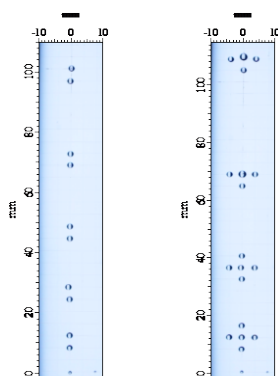


Fig. 1 Cluster configuration for the present experiments.

view could provide an image of both the flame and the droplet array. The backlight came on for approximately two video frames (0.0667 s), then turned off for four video frames (0.133 s) and the cycle repeated for the duration of the test.

The spatial resolution of the video images was low enough that the analysis tools used for previous droplet combustion experiments³⁰) would not work to measure droplet size. To measure the droplet size as a function of time in the present experiments we present a new technique that involved getting a line profile through the center of the droplet from a single video frame. Since the droplet appears as a dark circle on a light background the grayscale profile of a line through the droplet goes from high grayscale values to low grayscale values from the background to the droplet. The droplet diameter is simply the distance between the points on either side of the droplet line profile where the grayscale value is less than some threshold value of the difference between the background and droplet grayscale values. This results in diameter measurements that are of sub-pixel resolution and allow for better estimates of the burning rate constant. The technique works well for the largest droplets (2 mm), reasonably well for the intermediate droplets (1 mm) and did not work at all for the smallest droplets (0.7 mm).

For most of the burning history following a brief ignition transient, the droplets and clusters burn with a (presumably) dim blue flame that is mostly invisible to the video camera. The flame position and diameter are estimated by looking at the glow of the SiC fiber when the backlight is off. By looking at the the points along each fiber where the intensity reaches a maximum allows for an estimate of the flame position in that frame. Any time the hot flame impinges on the fiber the incandescence from the fiber registers on the video image (images with the backlight off). Ideally the flame is relatively symmetric about an axis in the direction of the flame spread so that if there is a hot flame there should be some record in the video footage. In most cases, this is what the video results show. Near hot-flame extinction, however, the flames can become unstable and oscillate and the flame is not symmetric. In this case there may be a hot flame present but it does not impinge on the fiber and therefore doesn't appear in the video image. In cases where this occurs there is some ambiguity as to whether a hot flame is present or not.

3. Experimental Results

The original goal of this experiment conducted in the GCEM was to investigate flame spread between droplet clusters. This report, however, focusses on the cool-flame burning that was observed during the experiments. Figure 2 shows a sample result for one of the tests. The left ordinal axis shows the droplet diameter squared and the right axis the flame position. There is a reference image for the cluster configuration to show the flame position relative to the array. The cluster closest to the igniter is designated C0 with C1, C2, etc. at increasing distance from the igniter. Within a given cluster the droplet D0 is closest to the igniter with D1 4 mm away at increasing distance from the ignition source. For the five-droplet clusters D0 is closest to the igniter and then D1, D2 and D3 further away from the igniter from left to right, respectively and D4 the furthest away from the igniter.

Fig. 2 shows that the flame quickly propagates through the first three clusters (C0, C1 and C2) with a relatively uniform speed of approximately 15 mm/s. The flame position then advances slowly until the next cluster, C3 ignites and the flame

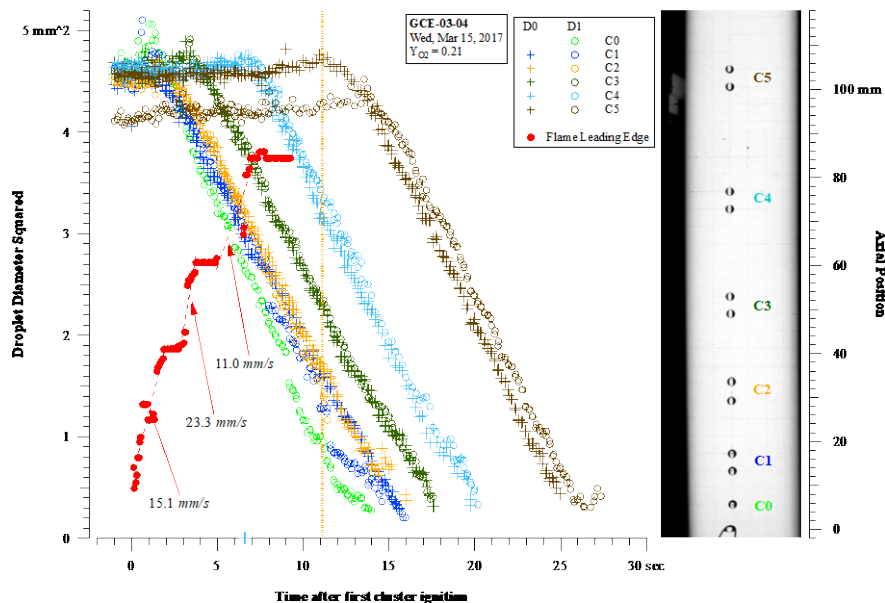


Fig. 2 Droplet histories and flame propagation of GCE-03-04.

moves quickly over that cluster. There is then a somewhat longer delay before cluster C4 ignites. The hot flame never ignites cluster C5 and there is no evidence of a hot flame after approximately 11 s (denoted by the vertical line in Fig. 1). The hot-flame extinction is almost certainly caused by the excessive radiative loss from the flame that decreases the flame temperature below the value (~ 1200 K) that can support a hot flame. We should note that the initial droplet sizes in this test (~ 2 mm) would burn to completion if they burned in an isolated environment. The droplet interactions in this case are clearly promoting radiative extinction.

The flame progression is clearly shown in the burning history for each of the droplets. The droplet history shows that prior to cluster ignition the droplet history is mostly flat, any vaporization either small or offset by the increasing droplet size due to the reduced liquid density. Coincident with the arrival of the flame the droplet begins to vaporize and the diameter squared decreases linearly until the droplet is smaller than can be resolved from the video images. Table 1 shows the burning rate constant resulting from a linear fit of the droplet history in Fig. 2. The data in Table 1 show that except for the C0-D1 droplet (cluster C0, droplet D1) which has a somewhat higher burning rate constant, the burning rates for all the droplets are very similar, well within the measurement errors associated with the droplet size estimates.

The results in Fig. 2 for this test also show that for more than half the test (assuming the test ends approximately 26 s after cluster C0 ignites when the droplets in cluster C5 disappear) there is no visible flame present. The results show that following ignition of a cluster the flame surrounding the cluster increases in size and gets dimmer (as judged by the grayscale of the glowing fiber). Eleven seconds after the first cluster ignites the hot flame extinguishes. When the hot flame extinguishes, however, only the droplets in cluster C0 have vaporized completely. While clusters C2 and C2 have mostly vaporized, cluster C3 is only halfway vaporized ($D^2 \sim 0.5D_0^2$) and cluster C4 is only one third through its burning history.

Based on previous ISS results⁷⁻¹⁰ the droplets in the clusters C1 - C4 continue to burn after hot-flame extinction, the burning sustained by a cool flame(s). The droplet history shows that the regression of the droplets, at least to the resolution from the video record, is not impacted by the hot-flame extinction. This is consistent with the cool-flame results from the ISS droplet combustion experiments that show cool-flame burning rate constants not that much different than the hot-flame burning rate constants (before radiative extinction)⁷⁻¹⁰.

The burning behavior of clusters C0-C4 are interesting, but not surprising based on previous ISS testing. The most unique finding of this test (and of the present experiments) is the behavior of cluster C5. The hot flame never propagates to cluster C5 as the distance between clusters C4 and C5 is too large. The droplet history shows, however, that the droplets

Table 1 Burning rate constants (mm^2/s) for the droplets in Fig. 2.

Cluster/Droplet	D0	D1
C0		0.41
C1	0.31	0.34
C2	0.34	0.37
C3	0.32	0.32
C4	0.34	0.34
C5	0.35	0.35

in C5 ignite and burn but with no hot flame (judging by the SiC fiber) ever present around the cluster. The only reasonable explanation is that while the distance between clusters C4 and C5 is too large for hot-flame spread, there is enough energy transport ahead of the hot flame to ignite cluster C5 to burn with a cool flame. We should note that this was not the only test where this behavior occurred as there were several tests where the last cluster burned with a cool flame without ever having a hot flame surround the cluster.

A closer examination of Fig. 2 suggests another unique observation, cool flame propagation between the droplets in the cluster. A reasonable assumption, backed by the experimental data, is that the droplet ignites shortly before, or coincident with, droplet regression (i.e., the droplet regression begins when it ignites). That is certainly the case for clusters C1 - C4. The droplet regression begins coincident with the flame surrounding the cluster. The regression histories for both droplets in these clusters is virtually identical, within the measurement uncertainty available from the video images. Cluster C5 is, however, different. The regression of droplet C5-D0 begins, not surprisingly, nearly coincident with hot-flame extinction. The regression of droplet C5-D1, however, does not begin until nearly 2 s after hot-flame extinction. These results imply that droplet D0 in C5 begins burning with a cool flame coincident with hot flame extinction and that cool flame ignites a cool flame around droplet D1 over 2 s later. We should note that while most of the ISS single droplet combustion experiments showed hot-flame radiative extinction with subsequent cool-flame burning a small number of experiments showed that cool-flame burning could be initiated without first igniting a hot flame³¹.

Subsequent tests with the same cluster configuration at ambient oxygen mole fractions of 0.19 and 0.17 showed similar behavior to the results in Fig. 1. The major difference was the progression of the hot flame. In the test described above the hot flame spread to cluster C4 then radiatively extinguished but ignited a cool flame around cluster C5. At an ambient oxygen mole fraction of 0.19 the hot flame spread to cluster C2 (an axial position of 60 mm) before radiatively extinguishing (approximately 7 s after cluster C0 ignition). Coincident with hot-flame extinction droplet D0 of cluster C3 ignited with a cool flame and then several seconds later droplet D1 in the cluster ignited and burned with a cool flame. The behavior at an ambient oxygen mole fraction of 0.17 was nearly identical except that only cluster C0 ignited and burned (briefly, approximately 2 s). Droplet D0 of cluster C1 ignites with a cool flame coincident with hot-flame extinction followed by ignition and cool-flame burning of droplet D1 over 4 s after hot-flame extinction.

The hot-flame burning times decrease significantly with decreasing ambient oxygen mole fraction, from 11 s at $X_{O_2} = 0.21$ to approximately 2 s at $X_{O_2} = 0.17$. This means that at the lowest ambient oxygen mole fraction almost all the droplets burn with a cool flame with almost not hot-flame burning. The other noteworthy observation at $X_{O_2} = 0.17$ is that the flame surrounding droplet D1 in cluster C1 appears to extinguish when droplet D0 completes burning. At this oxygen concentration the cool flame extinction droplet diameter for an isolated droplet is relatively large(ref). Therefore if droplet interactions promote cool flame burning then one would expect the cool flame around a droplet in an array to extinguish when the neighboring droplet is completely consumed if the droplet diameter is below the isolated droplet cool flame extinction droplet diameter.

The cool-flame burning rate constant for both droplets in cluster C5 is approximately $0.35 \text{ mm}^2/\text{s}$. This value is only about 10 percent lower than the cool flame burning rate constant for a single isolated droplet ($\sim 0.39 \text{ mm}^2/\text{s}$) observed in the ISS droplet combustion experiments^{7,8}). The cool-flame burning rate constant for an isolated droplet decreases to approximately $0.32 \text{ mm}^2/\text{s}$ when the X_{O_2} decreases to 0.17. The current experiments show that at $X_{O_2} = 0.17$ the burning rate constant for the two droplets in cluster C1 (that only exhibited cool flame burning) was $0.26 \text{ mm}^2/\text{s}$. This seems to suggest that the cool flame burning rate constant for the binary array has a slightly larger dependence on the ambient oxygen mole fraction than does the single droplet.

The behavior described above was for droplets with an initial droplet size of approximately 2 mm. For tests in the two-droplet cluster configuration with an initial droplet diameter of approximately 1 mm (the same configuration as in Fig. 2) the experiments showed similar behavior. That is the hot flame propagated and terminated at clusters C2, C1 and C1 for $X_{O_2} = 0.21, 0.19$ and 0.17 , respectively. The hot flame extinction in this case, however, was coincident with the droplet disappearance so the droplets that ignited with a hot flame burned to completion with a hot flame. While the hot flame stopped propagating it did initiate cool-flame burning of the next cluster in each of the X_{O_2} tests. So the hot flame igniting the cluster ahead into cool flame burning was prevalent in the two-droplet cluster experiments.

This hot flame igniting a cool flame ahead of it did not occur in the five-droplet cluster experiments. The hot flame surrounding the five-droplet clusters extinguished radiatively shortly after the flame spread to surround a cluster, especially for the tests with an initial size of 2 mm. The cool flame burning rate constants were lower than those observed in the two-droplet clusters. For the five-droplet cluster of 2 mm droplets at $X_{O_2} = 0.17$ the four droplets on the outside (D0, D1, D3 and D4) had a burning rate constant of approximately $0.22 \text{ mm}^2/\text{s}$ and the center droplet a value of approximately $0.18 \text{ mm}^2/\text{s}$. These were the lowest values observed in these GCE tests and show how interactions and lower oxygen ambient can combine to create very low cool-flame burning rates.

4. Conclusions

The experiments involved studying the flame spread between clusters of pure decane droplets with increasing distance between the clusters in the direction of the spread. The ambient atmospheres for the tests were oxygen/nitrogen mixtures with oxygen mole fractions of 0.17, 0.19 and 0.21 at 1 atm pressure. The results showed relatively fast uniform spread at small cluster separations followed by individual cluster ignition at larger distances and eventually a separation where the hot-flame propagation stopped completely. For the largest droplets ($D_0 = 2 \text{ mm}$) the hot flame quickly extinguished presumably from excessive radiant energy loss and this was followed by a prolonged period of cool-flame burning. For both the $D_0 = 1$ and 2 mm droplets in the two-droplet cluster experiments the experiments showed a distinct behavior

where the cluster ahead of the hot flame would ignite a cool flame even though the hot flame never ignited around the cluster. The droplets in this cluster would then burn to completion with a cool flame. The results further showed the apparent spread of a cool flame between droplets in a cluster.

5. References

- 1) G.A.E. Godsave: Proceedings of the Combustion Institute, **4**, (1952), 818.
- 2) S. Kumagai and H. Isoda: Proceedings of the Combustion Institute, **6**, (1956) 726.
- 3) M.Y. Choi and F.L. Dryer: Microgravity Combustion: Fire in Free Fall, Chapter 4, Academic Press (2001) 183.
- 4) A.J. Marchese and F.L. Dryer: Proceedings of the Combustion Institute, **26**, (1996) 1209.
- 5) A.J. Marchese, F.L. Dryer and V. Nayagam: Combustion and Flame, **116**, (1999) 432.
- 6) B.L. Zhang, J.M. Card and F.A. Williams: Combustion and Flame, **105**, (1996) 267.
- 7) V. Nayagam, D.L. Dietrich, P.V. Ferkul, M.C. Hicks and F.A. Williams: Combustion and Flame, **159**, (2012) 3583.
- 8) V. Nayagam, D.L. Dietrich, M.C. Hicks and F.A. Williams: Combustion and Flame, accepted for publication.
- 9) T.I. Farouk and F.L. Dryer: Combustion and Flame, **161**, (2014) 565.
- 10) A. Cuoci, A. Frassoldati, T. Faravelli and E. Ranzi: XXXVI Meeting of the Italian Section of the Combustion Institute (2013).
- 11) D.L. Dietrich, R. Calabria, P. Massoli, V. Nayagam and F.A. Williams: Combustion Science and Technology, **189**(3), (2017) 520.
- 12) K. Annamalai: Mechanics and Combustion of Droplets and Sprays, Begell House, Inc. (1995), 116.
- 13) D. Dunn-Rankin, W.A. Sirignano, R. Rangel and M. Orme: Mechanics and Combustion of Droplets and Sprays, Begell House, Inc., (1995) 74.
- 14) K. Miyasaka and C.K. Law: Proceedings of the Combustion Institute, **18**, (1981) 283.
- 15) T.Y. Xiong, C.K. Law and K. Miyasaka: Proceedings of the Combustion Institute, **20**, (1984) 1781.
- 16) M. Mikami, H. Kato, M. Kono and J. Sato: Proceedings of the Combustion Institute, **25**, (1995) 423.
- 17) M. Labowsky: Combustion Science and Technology, **22**, (1980) 217.
- 18) P.M. Struk, D.L. Dietrich, M. Ikegami and G. Xu: Proceedings of the Combustion Institute, 29.
- 19) D.L. Dietrich, V. Nayagam and F.A. Williams: Proceedings of the 9th U.S. National Combustion Meeting, Cincinnati, Ohio., (2015).
- 20) T.A. Brzustowski, A. Sobiesiak and S. Wojcicki: Proceedings of the Combustion Institute, **18**, (1981) 265.
- 21) T.A. Brzustowski, E.M. Twardus, S. Wojcicki and A. Sobiesiak: AIAA Journal **17**(11), (1979) 1234.
- 22) S. Kato, H. Mizuno, H. Kobayashi and T. Niioka: Fourth International Microgravity Combustion Science Workshop, NASA Conference Publication 10194, (1997).
- 23) M. Mikami, H. Oyagi, N. Kojima, M. Kikuchi, Y. Wakashima and S. Yoda: Combustion and Flame, **141**, (2005) 241.
- 24) M. Mikami, H. Oyagi, N. Kojima, Y. Wakashima, M. Kikuchi and S. Yoda: Combustion and Flame, **146**, (2006) 391.
- 25) H. Nomura, Y. Suganuma, A. Setani, M. Takahashi, M. Mikami and H. Hara: Proceedings of the Combustion Institute, **32**, (2009) 2163.
- 26) H. Nomura, M. Takahashi, Y. Ujiie and H. Hara: Proceedings of the Combustion Institute, **30**(2), (2005) 1991.
- 27) M. Mikami, M. Kikuchi, Y. Kan, T. Seo, H. Nomura, Y. Suganuma, O. Moriue and D.L. Dietrich: International Journal of Microgravity Science and Applications, **33** (2), (2016)
- 28) M. Mikami, H. Nomura, Y. Suganuma, M. Kikuchi, T. Suzuki and M. Nokura: International Journal of Microgravity Science and Applications, **35** (2), (2018)
- 29) M. Mikami, Y. Yoshida, T. Seo, T. Sakashita, M. Kikuchi, T. Suzuki and M. Nokura: Microgravity Science and Technology, **30**, (2018), 535–542.
- 30) P.M. Struk, M. Ackerman, V. Nayagam and D.L. Dietrich: Microgravity Science and Technology, **XI** (4), 144–151.
- 31) T.I. Farouk, D. Dietrich, F.E. Alam and F.L. Dryer: Proceedings of the Combustion Institute, **36**(2), (2017) 2523.

Notice for Copyrighted Information: This manuscript is a work of the United States Government authored as part of the official duties of employee(s) of the National Aeronautics and Space Administration. No copyright is claimed in the United States under Title 17, U.S. Code. All other rights are reserved by the United States Government. Any publisher accepting this manuscript for publication acknowledges that the United States Government retains a non-exclusive, irrevocable, worldwide license to prepare derivative works, publish or reproduce the published form of this manuscript, or allow others to do so, for United States government purposes.